



Research article

Arabidopsis thaliana GPAT8 and GPAT9 are localized to the ER and possess distinct ER retrieval signals: Functional divergence of the dilysine ER retrieval motif in plant cells

Satinder K. Gidda^a, Jay M. Shockey^b, Steven J. Rothstein^a, John M. Dyer^{c,**}, Robert T. Mullen^{a,*}

^a Department of Molecular and Cellular Biology, University of Guelph, Guelph, Ontario, Canada N1G 2W1

^b United States Department of Agriculture, Agricultural Research Service, Southern Regional Research Center, New Orleans, LA 70124, USA

^c United States Department of Agriculture, Agricultural Research Service, US Arid-Land Agricultural Research Center, Maricopa, AZ 85238, USA

ARTICLE INFO

Article history:

Received 2 December 2008

Accepted 27 May 2009

Available online 9 June 2009

Keywords:

Arabidopsis thaliana

Dilysine motif

Endoplasmic reticulum

Glycerol-3-phosphate acyltransferase

Lipids

Localization

Retrieval signal

ABSTRACT

Glycerol-3-phosphate acyltransferase (GPAT; EC 2.3.1.15) catalyzes the committed step in the production of glycerolipids, which are major components of cellular membranes, seed storage oils, and epicuticular wax coatings. While the biochemical activities of GPATs have been characterized in detail, the cellular features of these enzymes are only beginning to emerge. Here we characterized the phylogenetic relationships and cellular properties of two GPAT enzymes from the relatively large *Arabidopsis thaliana* GPAT family, including GPAT8, which is involved in cutin biosynthesis, and GPAT9, which is a new putative GPAT that has extensive homology with a GPAT from mammalian cells involved in storage oil formation and, thus, may have a similar role in plants. Immunofluorescence microscopy of transiently-expressed myc-epitope-tagged GPAT8 and GPAT9 revealed that both proteins were localized to the endoplasmic reticulum (ER), and differential permeabilization experiments indicated that their N- and C-termini were oriented towards the cytosol. However, these two proteins contained distinct types of ER retrieval signals, with GPAT8 possessing a divergent type of dilysine motif (–KK–COOH rather than the prototypic –KKXX–COOH or –KXKXX–COOH motif) and GPAT9 possessing a hydrophobic pentapeptide motif (– ϕ –X–X–K/R/D/E– ϕ –; where ϕ are large hydrophobic amino acid residues). Notably, the divergent dilysine motif in GPAT8 only functioned effectively when additional upstream residues were included to provide the proper protein context. Extensive mutational analyses of the divergent dilysine motif, based upon sequences present in the C-termini of other GPATs from various plant species, further expanded the functional definition of this molecular targeting signal, thereby providing insight to the targeting signals in other GPAT family members as well as other ER-resident membrane proteins within plant cells.

© 2009 Elsevier Masson SAS. All rights reserved.

Abbreviations: ACP, acyl-carrier protein; BY-2, Bright Yellow-2; Cf9, *Cladosporium fulvum*-9; ConA, concanavalin A; DIC, differential interference contrast; DGAT, diacylglycerol acyltransferase; ER, endoplasmic reticulum; FAD, fatty acid desaturase; GPAT, glycerol-3-phosphate acyltransferase; GFP, green fluorescent protein; LPAT, lysophosphatidic acid acyltransferase; MCS, multiple cloning site; ORF, open reading frame; RFP, red fluorescent protein; SNARE, soluble N-ethyl-maleimide sensitive factor attachment protein receptor; SRP, signal-recognition particle; TAG, triacylglycerol; TMD, transmembrane domain.

* Corresponding author. Tel.: +1 519 824 4120x56479.

** Corresponding author. Tel.: +1 520 316 6356.

E-mail addresses: john.dyer@ars.usda.gov (J.M. Dyer), rtmullen@uoguelph.ca (R.T. Mullen).

1. Introduction

Glycerolipids play an essential role in plant biology by serving as major components of cellular membranes, storage oils in developing seeds, and the protective, hydrophobic barrier on the cuticular surface of plant organs [41]. Glycerolipids and their associated metabolites also serve as part of the dynamic signaling processes associated with many aspects of plant growth and development and resistance to both biotic and abiotic stresses.

The production of glycerolipids in plant cells begins with the activity of a glycerol-3-phosphate acyltransferase (GPAT) enzyme, which catalyzes the transfer of a fatty acid from the acyl-CoA pool (or acyl-ACP pool in plastids) to the *sn*-1 position of glycerol-3-phosphate, resulting in formation of lysophosphatidic acid [38]. Subsequent acylation of lysophosphatidic acid at the *sn*-2 position by lysophosphatidic acid acyltransferase (LPAT) results in

production of phosphatidic acid, which is a key intermediate in the metabolic pathways responsible for both membrane polar lipid and neutral storage lipid biosynthesis [41]. Overall, the metabolic fate(s) of these glycerolipid metabolites is determined in part by the subcellular localization of the enzymatic reactions responsible for their production. For example, glycerolipids synthesized in chloroplasts are converted primarily to galactolipids, which serve as major structural and functional components of photosynthetic membranes [12]. Glycerolipids produced in the endoplasmic reticulum (ER), however, are converted primarily to cellular membrane phospholipids and, in developing seeds, to storage oil triacylglycerols (TAGs) [41]. Glycerolipid synthesis is known to occur also in mitochondria, and evidence from both mammals and plants suggests that this pathway also contributes to the synthesis of membrane lipids and several important aspects of TAG formation, such as the relative composition of TAGs in plant cells [62] and the formation of serum lipids in mammals [18].

Genes encoding membrane-bound GPAT activity were first identified in bacteria [59], and subsequently in mammals for mitochondrial-localized GPATs [18]. In plants, the first GPAT genes identified were those that encoded enzymes localized to plastids, which are soluble enzymes and, thus, facilitated their purification and gene cloning [38]. Comparative analysis of these soluble GPATs and other GPATs from evolutionarily diverse organisms has since revealed that all members of the GPAT superfamily contain at least four highly conserved amino acid sequence motifs that are essential for both acyltransferase activity and the binding of glycerol-3-phosphate substrate [27].

While it has long been recognized that GPAT enzyme activity is present also in ER microsomal preparations from yeast, plants and mammalian cells and that these activities contributed to both membrane lipid and storage lipid biosynthesis, the genes encoding these enzymes have only recently been identified. For instance, two microsomal GPAT enzymes termed GAT1 and GAT2 were identified in yeast [2,63], and more recently an enzyme termed GPAT3 was identified in mammalian cells [9]. Mammalian GPAT3 is particularly notable among the GPAT family because it is associated with storage oil formation in mammalian cells and is strongly induced during adipocyte differentiation [18]. In plants, a bioinformatics-based search of the *Arabidopsis* genome with the yeast GAT1 and GAT2 sequences revealed a family of eight related genes (termed GPAT1 through GPAT8) that encode proteins of similar size and amino acid sequence identity, including the four amino acid motifs that are characteristic of all members of the GPAT family [5,62]. Indeed, functional analysis of 7 of these 8 GPAT enzymes through heterologous expression in yeast cells demonstrated that at least 5 possess GPAT activity [62]. Moreover, characterization of GPAT1 revealed that it is localized to mitochondria in vitro and plays an essential role in pollen fertility [62]. GPAT4, 5 and 8, on the other hand, are involved in the production of suberin or cutin [5,28]. The subcellular localization of these latter three GPAT enzymes, however, has not been clearly defined. Furthermore, no gene(s) encoding GPAT activity involved in ER-localized storage oil production in plants has been identified.

We are interested in the cellular and organizational properties of lipid-metabolic enzymes in plant cells, with an emphasis on those enzymes involved in storage oil production in the ER. Towards this end, we previously characterized the fatty acid desaturase and diacylglycerol acyltransferase enzymes from *Arabidopsis* and/or tung (*Vernicia fordii*), the latter of which catalyze the committed step in storage oil formation [13,14,32,54]. Here, we describe the cellular properties of several GPAT enzymes, using the *Arabidopsis* GPAT enzyme family as a model system, including the subcellular localization and topological orientation of the GPAT8 protein. We also describe the identification of a new putative GPAT gene from *Arabidopsis* (At5g60620), referred to here as GPAT9,

which was identified through homology-based searches using the recently identified mammalian GPAT3 gene [9] as a probe.

Overall, we show that *Arabidopsis* GPAT8 and GPAT9 are both localized to the ER and exhibit a similar topological orientation in ER membranes, but that they contain distinct types of ER retrieval sequences. Further characterization of the ER retrieval signals in other members of the plant GPAT8 gene family allowed us to significantly expand the functional definition of dilysine-type targeting signals in plants. The implications of these results in terms of our understanding of ER protein trafficking in plant cells and the regulation of glycerolipid biosynthesis by GPATs located in different subcellular organelles in plants, compared to other evolutionarily diverse organisms, are discussed.

2. Results and discussion

2.1. Sequence analysis of the *Arabidopsis* GPAT family – identification of GPAT9

As mentioned in the Introduction, GPAT enzyme activity in *Arabidopsis* is encoded by a relatively large gene family containing at least eight members [5,62]. As shown in Fig. 1, alignment of the deduced polypeptide sequences of these GPAT proteins (GPAT1–8) demonstrates that they are similar in length and share several features that are characteristic of other membrane-bound GPATs from evolutionarily diverse organisms, including the presence of one or more predicted TMDs and four conserved amino acid motifs (Blocks I–IV) known to be important for acyltransferase activity [27]. The GPAT protein sequences also show a modest amount of sequence similarity (18% identical, 40% similar) with the highest degree of conservation detected in their C-terminal halves near the putative active sites (Fig. 1). The GPAT1 protein also possesses an extended N-terminal region that exhibits characteristics of a mitochondrial targeting peptide (albeit weakly detected by web-based protein targeting signal algorithms; data not shown), which is consistent with its reported localization to mitochondria in vitro [62]. All of the other GPAT proteins (GPAT2–8) lack any recognizable N-terminal intracellular targeting signal motifs, but do contain putative C-terminal ER retrieval signals (see below, Section 2.4).

Recent identification of an ER-localized GPAT protein in mammals (GPAT3) [9] provided an opportunity to identify a similar gene(s) in plants. Towards this end, we utilized a bioinformatics approach to identify a potential homolog of mammalian GPAT3 in *Arabidopsis* (see Materials and Methods for details). Referred to here as GPAT9, this putative mammalian GPAT3 homolog corresponds to locus number At5g60620 in the *Arabidopsis* genome database. Analysis of the encoded polypeptide sequence of GPAT9 reveals the presence of three predicted TMDs and all four conserved GPAT-type domains, but notably, the overall length of the protein (376 amino acids) is significantly shorter than that of other *Arabidopsis* GPAT family members (Fig. 1). Furthermore, the GPAT9 polypeptide sequence shares just 3% identity and 17% similarity with the GPAT1–8 consensus sequence, suggesting that it is distantly related to these GPATs.

To determine the evolutionary relationships of this newly-identified GPAT9 gene relative to other members of the *Arabidopsis* GPAT family, as well as to other GPAT genes from other organisms and that are well characterized in the literature, we performed a phylogenetic analysis. As shown in Fig. 2A, *Arabidopsis* GPAT9 is more closely related to the mammalian ER-localized GPAT3 and GPAT4 enzymes than it is to other members of the *Arabidopsis* GPAT family (GPATs 1–8), suggesting that the divergence of the GPAT9 gene from the GPAT1–8 family of *Arabidopsis* occurred prior to the evolutionary split between plants and mammals. The involvement of mammalian GPAT3 and GPAT4 in the production of storage TAG

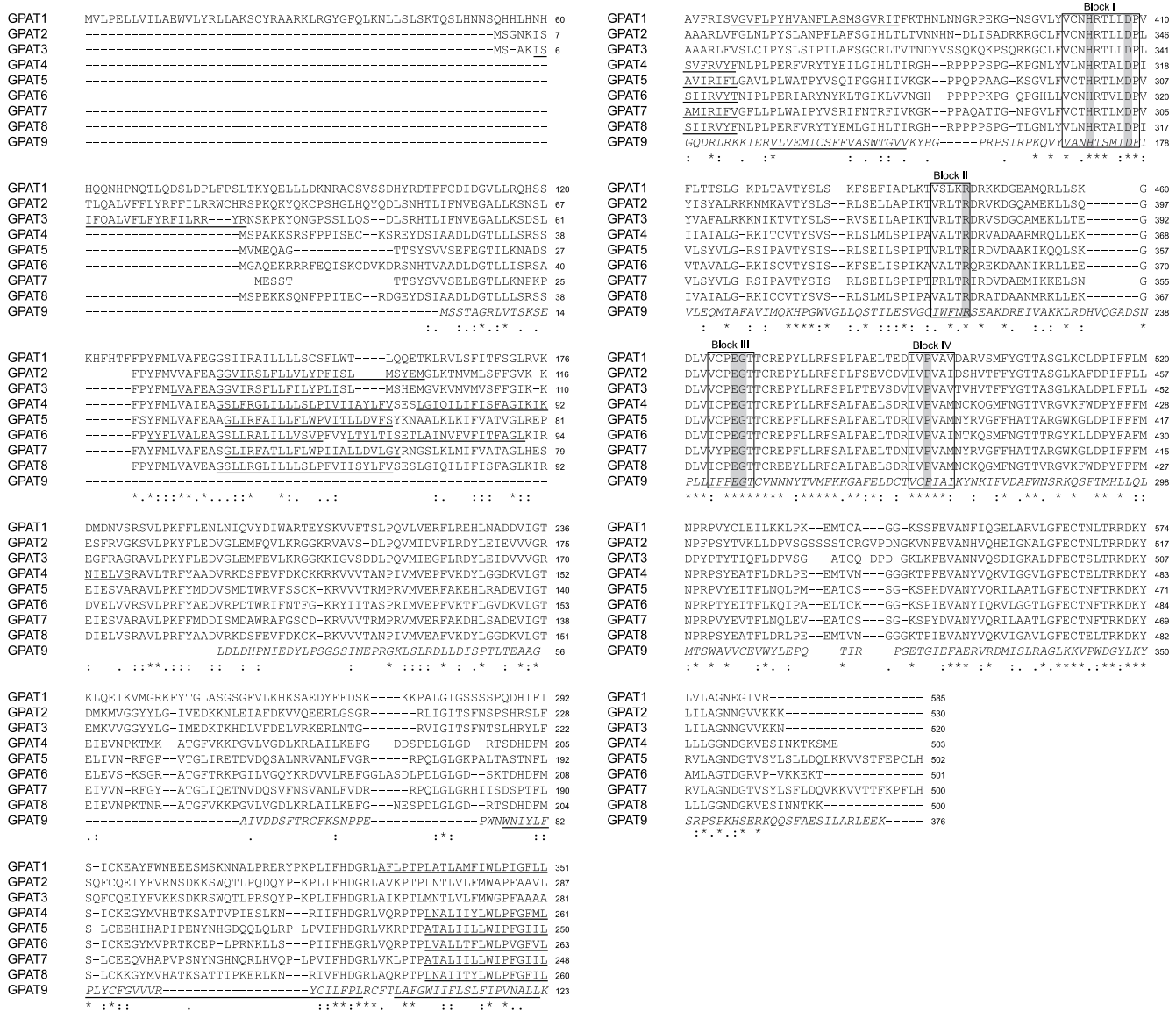


Fig. 1. Alignment of *Arabidopsis* GPAT proteins (GPAT1–9) and identification of conserved amino acid motifs. The protein sequences were aligned and compared as described in Materials and Methods. Putative TMDs are underlined. The four conserved acyltransferase superfamily motifs (Blocks I–IV) are boxed, and included in these motifs are residues previously shown to be critical for enzyme catalysis and substrate binding (highlighted grey) [27]. Note that for GPAT1–8 proteins only (i.e., not including GPAT9, which is italicized), identical amino acid residues in each protein are indicated by asterisks, and highly similar and similar residues are indicated with colons and periods, respectively.

in adipocytes [18] suggests also that *Arabidopsis* GPAT9 might play a similar role in glycerolipid metabolism in plant cells. While the function of the GPAT9 gene is currently unknown, the sequence of the encoded GPAT9 polypeptide is highly conserved (50% identical, 74% similar) for at least 16 different plant species (see Supplemental Fig. 1), suggesting that this gene likely plays an essential role(s) in plant lipid metabolism.

The phylogenetic analysis presented in Fig. 2A also demonstrates that the *Arabidopsis* GPAT1 protein, which was previously shown to be associated with mitochondria in vitro [62], is more similar to other members of the *Arabidopsis* GPAT family than it is to the mitochondrial GPATs identified in mammals. These results indicate that GPAT activity associated with mitochondrial glycerolipid metabolism has evolved multiple times in plants and mammals. In addition to the sequence divergence exhibited among the various GPAT proteins presented in the tree, the GPATs from different organisms (and different subcellular locations) also exhibited some differences in domain organization (Fig. 2B). For instance, the GPAT

enzymes located in mitochondria in mammalian cells (MmGPAT1 and MmGPAT2) each possess several putative TMDs that are located on different sides of the acyltransferase domain relative to the ER-localized proteins (mammalian GPAT3 and 4, and *Arabidopsis* GPAT8 and 9), suggesting that the topology of these proteins might be different. All of the *Arabidopsis* GPAT proteins (AtGPAT1–9) have a domain organization that is more similar to the ER-localized GPAT proteins from mammalian cells (MmGPAT3 and MmGPAT4), with the presence of one to three TMDs located N-terminally with respect to their acyltransferase domains. By contrast, the GPAT proteins located in plant plastids (not shown in Fig. 2) lack any TMDs altogether, but do contain predicted chloroplast transit peptides for transport of the proteins into the chloroplast stroma [38].

The identification of *Arabidopsis* GPAT9 as a new and potentially important member of the plant GPAT family is supported by digital (electronic) northern analysis of the *Arabidopsis* transcriptome. Specifically, searches of publicly available microarray datasets to uncover the expression profiles of the *Arabidopsis* GPAT gene family

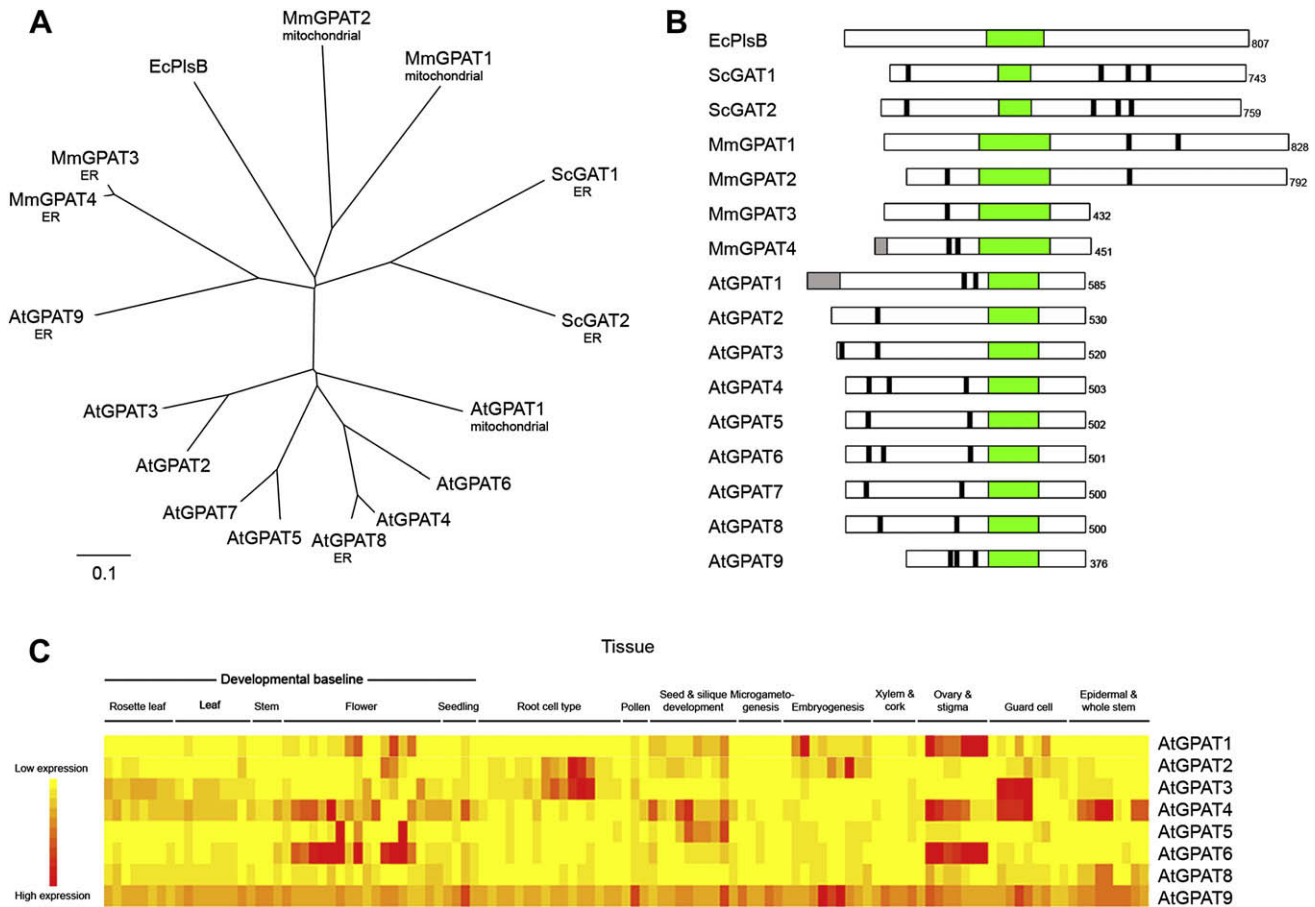


Fig. 2. Phylogenetic analysis, domain organization, and gene expression patterns of *Arabidopsis* GPATs. (A) Phylogenetic analysis of various GPAT sequences from *Arabidopsis thaliana* (At), *Saccharomyces cerevisiae* (Sc), *Escherichia coli* (Ec) and *Mus musculus* (Mm). The branch lengths of the tree are proportional to divergence and the 0.1 scale represents a 10% change. Also indicated for some GPAT proteins are their reported (either here for AtGPAT8 and AtGPAT9, or elsewhere for AtGPAT1 [62], MmGPAT1–4 [18] and ScGAT1 and ScGAT2 [2,63]) intracellular localization as ER or mitochondrial; the intracellular localization(s) of the other GPAT proteins shown in the tree is unknown. (B) Models depicting domain organization of GPAT proteins from various species shown in (A). Regions in each GPAT protein representing a predicted TMD (based on TMHMM Server v. 2.0) and the conserved acyltransferase domain (PF01553) are colored black and green, respectively. The putative N-terminal mitochondrial targeting peptide in MmGPAT4 and AtGPAT1 is colored grey. Also indicated is the total number of amino acid residues in each GPAT protein. Models depicting the domain organization of MmGPAT1–4 and ScGAT1 and 2 are based on models presented in [18] and [63], respectively. (C) Expression profiles of selected *Arabidopsis* GPAT genes in different tissues. To visualize the expression of the *Arabidopsis* GPATs in various tissue types, electronic (e)-northern analyses of the *Arabidopsis* transcriptome were conducted using the BioArray Resource (BAR) Expression Browser [57] and the AtGenExpress_Plus extended tissue series microarray dataset [48]. Expression values were retrieved and formatted using the DataMetaFormatter hosted at the BAR website. E-northern data for AtGPAT7 (At5g06090) was not included since this gene is not present on the ATH1 whole genome chip. (For interpretation of colors in the figure legend, the reader is referred to the web version of the article.)

(with the exception of GPAT7, which is not present on the ATH1 whole genome chip) revealed that the GPAT9 gene is indeed a functional gene that is expressed in a wide range of tissues and developmental stages (Fig. 2C). The levels of gene expression and tissue specificity are distinct from the other GPAT family members, which is consistent with the more diverged nature of the GPAT9 gene. Notably, the GPAT9 gene is significantly upregulated during embryogenesis, supporting a potential role for this GPAT in glycerolipid metabolism occurring in developing seeds, although this possibility remains to be tested experimentally.

2.2. *Arabidopsis* GPAT8 and GPAT9 localize to the ER in tobacco BY-2 cells

While the genetic, physiological and biochemical properties of several GPATs have recently been defined [5,28,62], the cellular details of these enzymes are only beginning to emerge. Thus, to increase our understanding of GPAT cellular organization and biogenesis, we conducted a detailed analysis of the localization and protein targeting mechanisms of GPAT8 and GPAT9 proteins from

Arabidopsis. The GPAT8 protein was selected for this study because it has been assigned a clear physiological role in cutin biosynthesis [28] and is related, albeit distantly, to the newly-identified putative GPAT9 protein. The subcellular localization of the GPAT8 and GPAT9 proteins was determined using tobacco (*Nicotiana tabacum*) Bright Yellow-2 (BY-2) suspension-cultured cells as a well-characterized *in vivo* protein import system [8,34,39]. Specifically, BY-2 cells were transiently transformed (via biolistic bombardment) with plasmid DNA encoding either GPAT8 or GPAT9 fused to the myc-epitope recognition motif (–EQKLISEEDL–; [16]) and, then, following a ~4 h incubation period to allow for gene expression and protein sorting, cells were processed for indirect immunofluorescence microscopy. The myc epitope was fused to the N terminus of GPAT8 (myc-GPAT8) or GPAT9 (myc-GPAT9) rather than the C terminus, since it was previously demonstrated that addition of an epitope tag to the N terminus of either human or mouse GPAT3 protein did not disrupt enzyme activity, and the epitope was further utilized to demonstrate the subcellular localization of these proteins to the ER in mammalian COS-7 cultured cells [9]. The usage of a myc-epitope tag with *Arabidopsis* GPAT8 and GPAT9 also allows for the

immunodetection of these transiently-expressed proteins relative to endogenous tobacco GPAT enzymes, whose partial sequences available in public databases show extensive sequence similarity when compared to the respective *Arabidopsis* proteins (data not shown). Notably, microscopic analyses of transformed BY-2 cells were performed at ~4 h after bombardment to ensure that any

potential negative effects on organelle morphology due to (membrane) protein expression were diminished [23,37,54].

Fig. 3 shows that both myc-GPAT8 and myc-GPAT9 displayed mostly reticular fluorescence patterns in BY-2 cells that colocalized with the fluorescence patterns attributable to endogenous ER stained with fluor-conjugated concanavalin A (ConA), a commonly

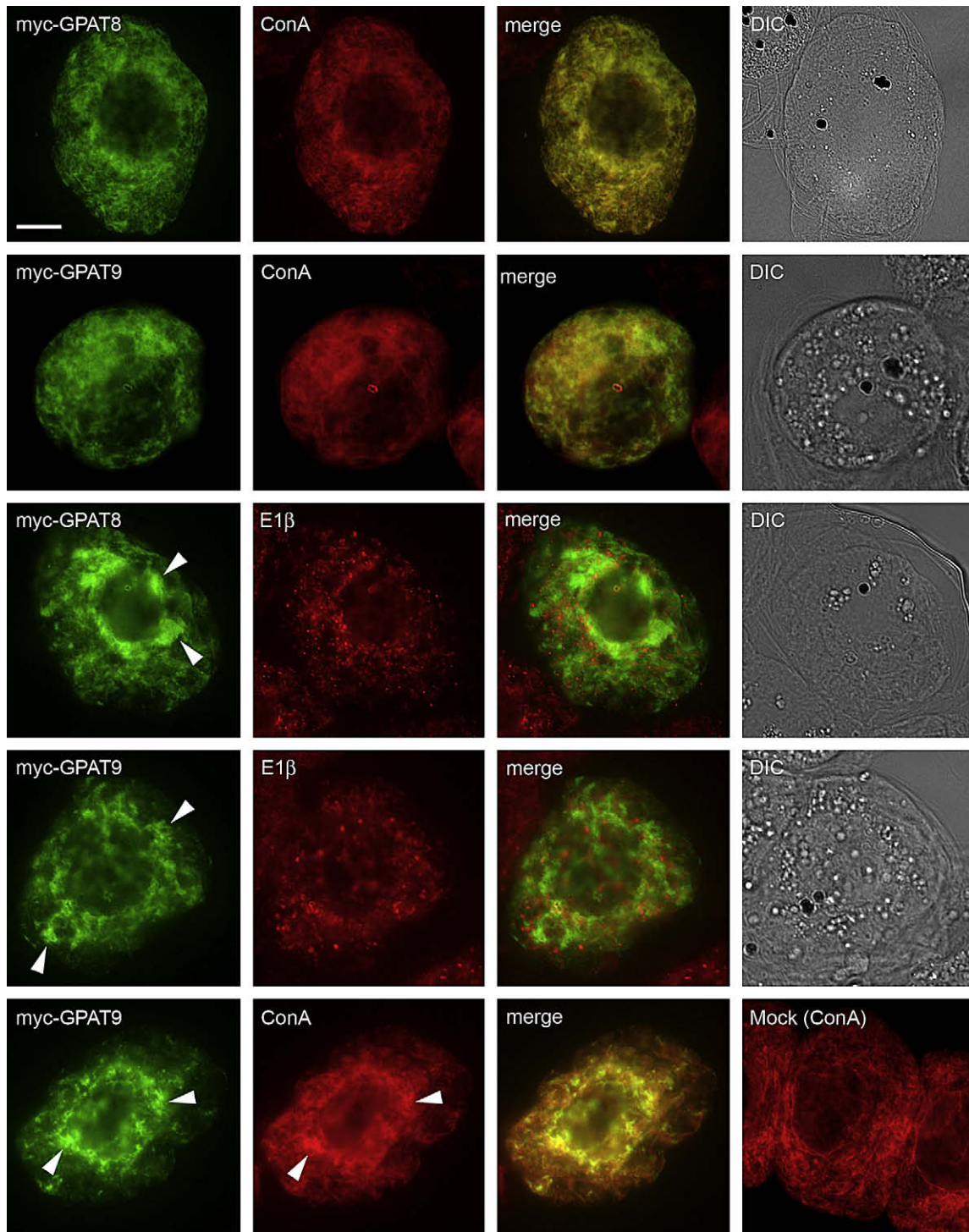


Fig. 3. Immunolocalization of N-terminal myc-tagged *Arabidopsis* GPAT8 and GPAT9 to the ER in transiently-transformed tobacco BY-2 suspension cells. Note the different appearance of the ER (i.e., a more globular morphology) in some of the myc-GPAT9-transformed cells (bottom two rows), as well as in the myc-GPAT8-transformed cell, co-stained with E1 β antibodies (middle row); arrowheads indicate obvious examples of ER with a different (globular) appearance in these cells. Note also the appearance of concanavalin A (ConA)-stained ER with a typical (reticular) appearance in mock-transformed cells (bottom row). Shown also are differential interference contrast (DIC) images of all myc-GPAT8- or myc-GPAT9-transformed cells, with the exception of the myc-GPAT9-transformed cell shown in the bottom row. Bar = 10 μ m.

used stain for the ER [55]. By contrast, neither myc-GPAT8 nor myc-GPAT9 colocalized with endogenous E1 β (Fig. 3), a protein subunit of the pyruvate dehydrogenase complex located in the mitochondrion [29], indicating that the subcellular localization of these two GPAT enzymes, and hence their physiological functions, are possibly distinct from that of mitochondrial-localized *Arabidopsis* GPAT1 [62]. Notably, GPAT8 and GPAT9 were also localized to the ER when the myc-epitope sequence was fused to their C-termini (GPAT8-myc and GPAT9-myc; see Fig. 4A below) and the addition of the myc tag or GFP to the N terminus of GPAT8 or GPAT9 proteins from tung tree (*V. fordii*) also resulted in the localization of these proteins to the ER (data not shown). Taken together, these data and those presented in Fig. 3 indicate that the addition of an epitope tag (or GFP) to the N (or C) termini of the GPAT proteins does not affect their normal subcellular targeting. Indeed, as mentioned above, a similar immuno-based epitope-tagging method has been employed to assess the subcellular localization of mammalian GPAT3 [9], as well as several other types of plant lipid biosynthetic enzymes [13,14,23,32,54], and in all cases the localization of these epitope-tagged proteins was

considered to faithfully reflect that of their endogenous (non-tagged) protein counterparts.

It is also notable that myc-GPAT9 frequently displayed a more globular fluorescence pattern compared to myc-GPAT8 in transformed BY-2 cells. That is, in ~40% of the myc-GPAT9-transformed cells, the protein often localized to globular structures in the perinuclear region that, because they were also co-stained with ConA, are likely ER with an altered (i.e., aggregated) morphology (cf. myc-GPAT9-transformed cells co-stained with ConA or E1 β and the mock-transformed cells stained with ConA; Fig. 3). While similar globular ER structures were observed in ~15% of cells expressing myc-GPAT8 (cf. myc-GPAT8-transformed cells co-stained with ConA or E1 β ; Fig. 3), but not in mock- or non-transformed cells (Fig. 3, bottom row), these results for myc-GPAT9 are consistent with the changes in ER morphology reported previously for the ectopic expression of mammalian GPAT3 in COS-7 cells [9]. However, whether these shared changes in ER morphology are due to some physical aspect of the expressed GPAT9 and GPAT3 protein structures, and/or the presence of their lysophosphatidic acid products in ER membranes, or, alternatively, are simply the consequence of the (over)expression of

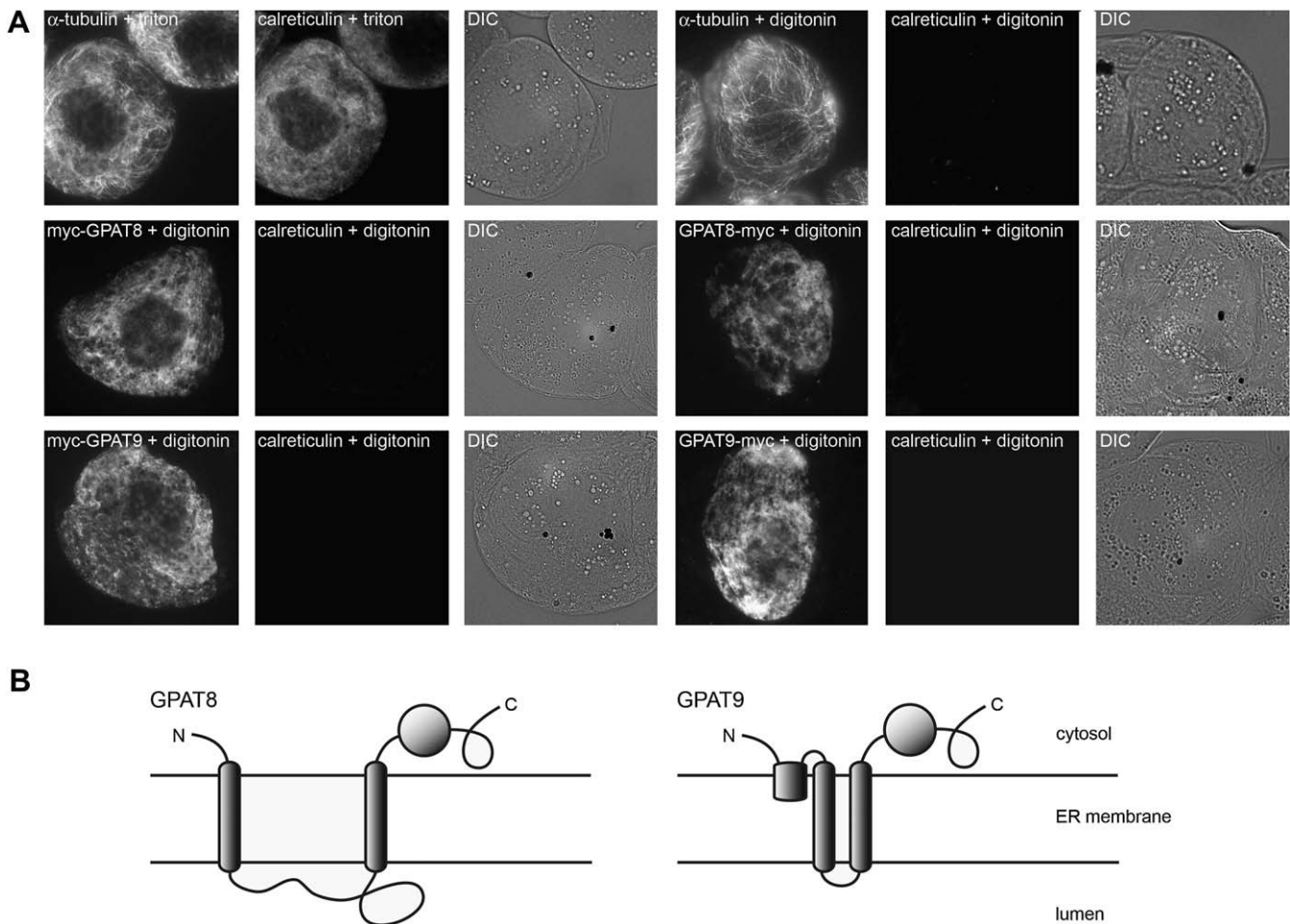


Fig. 4. Topological mapping of *Arabidopsis* GPAT8 and GPAT9 proteins in tobacco BY-2 suspension cells. (A) The presence or absence of immunofluorescence illustrates the membrane topology of transiently-expressed N- and C-terminal epitope-tagged GPAT proteins in differential-permeabilized BY-2 cells. Non-transformed (top row) or transiently-transformed (middle and bottom rows) cells were fixed and permeabilized with either triton X-100, which perforates all cellular membranes, or digitonin, which selectively permeabilizes the plasma membrane, then cells were processed for immunofluorescence microscopy. Note that both endogenous α -tubulin in cytosolic microtubules and calreticulin in the lumen of the ER were immunostained in the same non-transformed, triton X-100-permeabilized cells. By contrast, endogenous α -tubulin, but not calreticulin, was immunostained in the same digitonin-permeabilized cells. Note also that expressed myc-GPAT8, myc-GPAT9, GPAT8-myc and GPAT9-myc, but not endogenous calreticulin, were immunostained in the same digitonin-permeabilized cells, demonstrating that both the N- and C-termini of GPAT8 and GPAT9 are located in the cytosol. Shown also are DIC images of all non-transformed and myc-GPAT8- or myc-GPAT9-transformed cells. Bar = 10 μ m. (B) Topology model for GPAT8 and GPAT9 proteins located in the ER. Each protein is anchored in the membrane by two TMDs, with the additional (N-terminal) hydrophobic region predicted for GPAT9 (see Fig. 1) partially spanning (or peripherally associated with) the ER membrane. The C-terminal active site of each enzyme (depicted as a circle) is located on the cytosolic side of the membrane.

certain lipid biosynthetic-related ER membrane proteins as reported elsewhere (e.g., Ref. [13]) remains to be determined.

2.3. Both GPAT8 and GPAT9 are oriented in the ER membrane with their N- and C-termini facing the cytosol

Sequence analysis of GPAT8 and GPAT9 proteins revealed the presence of four highly conserved amino acid motifs in the C-terminal half of the proteins that were previously shown to be essential for acyltransferase activity and the binding of glycerol-3-phosphate substrate [27] (refer to Figs. 1 and 2B). There are also a number of predicted TMDs present upstream of the active site in the N-terminal half of the proteins (Fig. 2B), suggesting that GPAT8 and GPAT9 proteins are anchored to ER membranes with these N-terminally positioned TMDs, and the C-terminal active site located entirely on one side of the ER membrane or the other.

To determine the topology of the GPAT8 and GPAT9 proteins with respect to ER membranes we employed a differential detergent permeabilization assay [26], wherein BY-2 cells were transformed transiently with N- or C-terminal myc-tagged versions of these enzymes and then fixed and incubated either with digitonin, which perforates only the plasma membrane, or triton X-100, which perforates all cellular membranes. Permeabilization with digitonin reveals only those epitopes exposed in the cytosol, whereas triton X-100 reveals epitopes present on both sides of cellular membranes [26]. As shown in Fig. 4A (top row), control experiments performed with non-transformed cells permeabilized with triton X-100 verified that endogenous proteins located in the cytosol (i.e., α -tubulin subunits of cytosolic microtubules) or within subcellular compartments (i.e., calreticulin in the ER lumen) can be detected under this condition, whereas permeabilization with digitonin allowed for the immunodetection of only cytosolic proteins (i.e., α -tubulin, but not calreticulin). When cells were transformed with N-terminally myc-tagged GPAT8 or GPAT9, the myc tag was immunodetected in cells permeabilized with either triton X-100 (data not shown) or digitonin (Fig. 4A), indicating that the N termini of these proteins were exposed to the cytosol. Similar results were observed when cells were transformed with C-terminally myc-tagged GPAT8 and GPAT9 proteins (Fig. 4A), indicating that the C terminus of each protein was also exposed to the cytosol.

The exposure of both the N- and C-termini of GPAT8 and GPAT9 to the cytosol (Fig. 4A) indicates that the proteins must have an even number of TMDs. Taken together with the data shown in Figs. 1 and 2B, which depicts two predicted TMDs present within GPAT8 and three TMDs within GPAT9, the most plausible model for the topological orientation of these two proteins in ER membranes is one that contains the following four features (Fig. 4B): (i) both the N- and C-termini are located in the cytosol; (ii) two TMDs serve to anchor the proteins in the ER membrane; (iii) the additional (third) hydrophobic region located towards the N terminus of GPAT9 does not span the membrane, but, rather may partially span (or peripherally associate with) the ER membrane, perhaps due to the presence of several proline residues that could induce the formation of a hinged or kinked region in this protein segment [10]; (iv) and the active site of the enzyme (containing the four conserved amino acid motifs) is located in the cytosolic-exposed C-terminal half of the protein.

Notably, the only other membrane-bound GPAT protein that has been carefully analyzed by topology mapping is the mammalian (mouse) mitochondrial GPAT1 protein [20]. Although this protein has TMDs positioned on the C-terminal side relative to the active site acyltransferase motifs (Fig. 2B), topology mapping revealed that this protein (similar to plant GPATs 8 and 9 shown here) also has both its N- and C-termini located towards the cytosol, which places the active site of the enzyme on the cytosolic side of the

membrane. It appears, therefore, that despite the apparent differences in positioning of TMDs in the plant GPAT8 and GPAT9 and mammalian GPAT1 proteins relative to their active sites, as well as their localization to different subcellular compartments, these proteins each adopt a similar overall topology with respect to cellular membranes. These observations also suggest that the acyltransferase reactions catalyzed by these particular GPAT proteins occur on the outer leaflet of the lipid bilayer in both subcellular compartments, i.e., ER and mitochondria. Moreover, it is interesting to note that the C-terminal end of the mammalian GPAT1 protein has been shown to physically interact with the N-terminally positioned acyltransferase domain, and that this interaction is essential for enzyme activity [44]. Whether a similar structural relationship exists between the N- and C-terminal regions of plant ER-localized acyltransferases remains to be determined.

2.4. Identification of distinct ER retrieval signals in GPAT8 and GPAT9 proteins

The steady-state localization of membrane proteins in the ER requires specific molecular signals for both their initial insertion into ER membranes and subsequent retention in the ER. For the majority of ER-localized membrane-bound proteins, insertion into ER membranes is mediated by the signal-recognition particle (SRP)/Sec61 co-translation/translocation pathway [49,51]. That is, once these proteins' first TMD sequence exits the ribosome during translation in the cytosol, it is recognized and bound by SRP, which halts translation until the entire SRP-TMD-ribosomal ternary complex is transported to and docks on the surface of ER membranes. Concomitantly, translation resumes and the TMD sequence is released from SRP and subsequently serves to anchor the protein in the ER membrane. The newly-synthesized and assembled ER membrane protein must then rely on one or more additional mechanisms to ensure its steady-state residency in the ER, since by default, proteins are generally secreted to post-ER compartments (e.g., Golgi). All such retention mechanisms are mediated by specific signals that direct either the retrieval of the ER-resident membrane protein back to the ER if it 'escapes' to a post-ER compartment, or the static retention of the ER-resident membrane proteins via protein-protein interactions.

Based on these current paradigms of ER membrane protein biogenesis, it is likely that the insertion of *Arabidopsis* GPAT8 and GPAT9, similar to nearly all other resident ER membrane proteins, is dependent upon their first hydrophobic TMD serving as an N-terminal signal/anchor sequence and the SRP/Sec61p translocon machinery. Likewise, the exposure of the N- and C-termini of GPAT8 and GPAT9 proteins to the cytosol (Fig. 4B) suggests that these proteins contain one or more of the cytoplasmically-exposed retrieval signals typically found in other ER-resident membrane proteins, including the best characterized of these signals, the C-terminal dilysine motif (-KKXX or -KXKXX) [19,43,56]. These motifs are recognized by type I coatomer (COPI) proteins at the surface of the *cis*-Golgi, which subsequently mediates the loading of the bound proteins into vesicles for retrograde transport back to the ER [25,33]. Indeed, inspection of the C-terminal sequences of *Arabidopsis* GPAT8 and GPAT9 revealed that at least GPAT8 contains a putative dilysine sequence at the -1, -2 position (-KK-COOH) (Fig. 5A), although this sequence does not match the originally defined consensus dilysine motif sequences -KXKXX-COOH or -KKXX-COOH (where two lysine residues are found at either the -3 and -5, or -3 and -4 positions) [24,40,53]. Similarly, dilysine-like sequences are present at the same or different positions within the C-termini of many other plant GPAT8 proteins (underlined sequences in Fig. 5A; refer also to Supplemental Fig. 2).

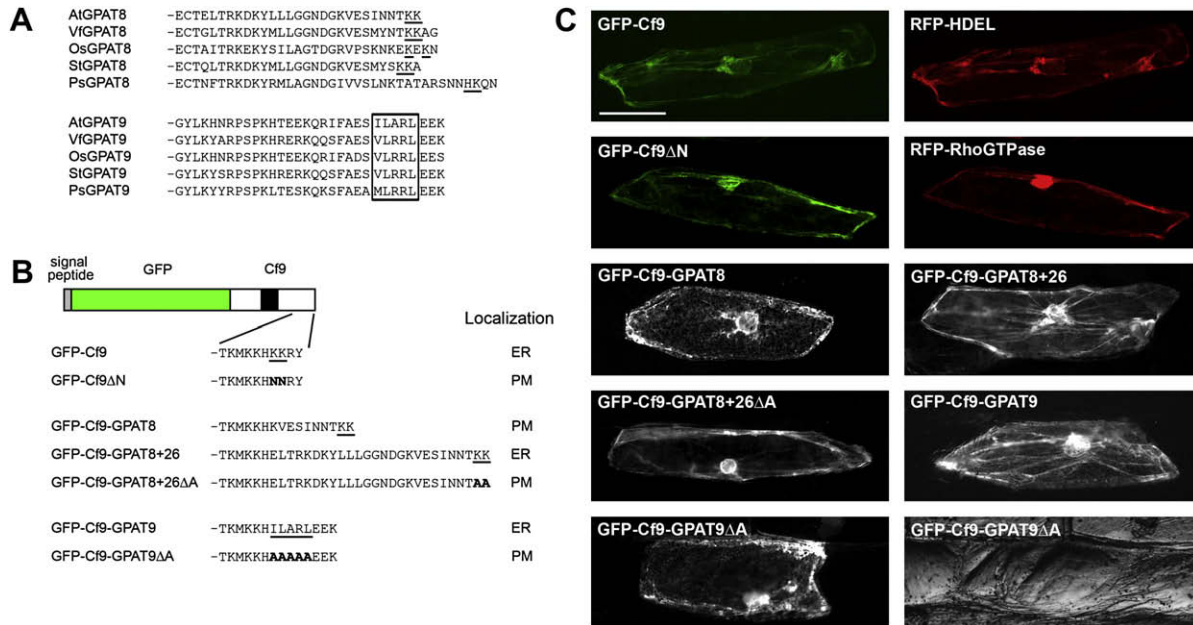


Fig. 5. Localization of various GFP-Cf9 fusion proteins in onion epidermal cells. (A) Deduced C-terminal amino acid sequence alignments of GPAT8 and GPAT9 proteins from various plant species including *Arabidopsis* (At), tung (Vf), rice (Os), potato (St) and pea (Ps). The lysine-like and hydrophobic pentapeptide-like ER retrieval motifs in GPAT8 and GPAT9 proteins are underlined and boxed, respectively. (B) Schematic representation of the GFP-Cf9 reporter fusion protein and the corresponding C-terminal sequences and intracellular localization (either ER or plasma membrane, PM) of GFP-Cf9 and modified versions thereof in transformed onion epidermal cells. The GFP-Cf9 chimeric reporter protein [6] consists of an N-terminal *Arabidopsis* chitinase signal peptide (grey box), the GFP (green box) and C-terminal amino acid sequences from Cf9 (open box) including the protein's single TMD (black box) and dilysine ER retrieval motif (underlined). The C-terminal GFP-Cf9 sequences were modified by replacing the protein's dilysine motif with either the *Arabidopsis* GPAT8 or GPAT9 C-terminal sequences, including each protein's putative dilysine or pentapeptide ER retrieval motifs (underlined). Modified amino acid residues in the various GFP-Cf9 or GFP-Cf9-GPAT8/GFP-Cf9-GPAT9 chimeric proteins are in bold letters. (C) Onion epidermal peels were (co-)transformed with different GFP-Cf9 chimeric proteins as illustrated in (B) and either RFP-HDEL, an ER marker protein [22], or RFP-RhoGTPase, a plasma membrane marker protein [7]. Following bombardment, peels were incubated for ~8 h in the dark and then visualized using either fluorescence or brightfield microscopy. Shown are representative individual onion cells (co-)expressing either GFP-Cf9 and RFP-HDEL, GFP-Cf9ΔN and GFP-RhoGTPase, GFP-Cf9-GPAT8, GFP-Cf9-GPAT8+26, GFP-Cf9-GPAT8+26ΔA, GFP-Cf9-GPAT9 or GFP-Cf9-GPAT9ΔA. Shown also is the corresponding brightfield image of the GFP-Cf9-GPAT9ΔA-transformed cell. Bar = 100 μm. (For interpretation of colors in the figure legend, the reader is referred to the web version of the article.)

Arabidopsis GPAT9 and other members of the GPAT9 protein family, however, do not contain a prototypic C-terminal dilysine sequence. Instead, these proteins all possess a pentapeptide sequence within their C-termini (boxed, Fig. 5A; refer also to GPAT9 sequences shown in Supplemental Fig. 1) that matches a recently characterized hydrophobic pentapeptide ER retrieval motif ($-\phi-X-X-K/R/D/E-\phi-$; where ϕ are large hydrophobic amino acid residues) [32]. Initially shown to function in the localization of at least a few yeast and mammalian ER-resident membrane proteins [11,30,31], the C-terminal hydrophobic pentapeptide ER retrieval motif was subsequently identified in plant fatty acid desaturases and diacylglycerol acyltransferases (DGATs) [32,54]. Extensive mutational analyses of this signal from plant fatty acid desaturases and DGATs also revealed the precise nature of this sequence-specific motif ($-\phi-X-X-K/R/D/E-\phi-$) [32] and that, unlike the originally defined motif in yeast and mammals, it can function upstream from the extreme C terminus [54].

To test whether the C-terminal dilysine and pentapeptide sequences of GPAT8 and GPAT9, respectively, function in maintaining their steady-state localization in the ER, we used the GFP-Cf9 reporter protein and onion epidermal cells as a well-characterized model system for studying protein sorting within the secretory pathway in plant cells [6,50]. As illustrated in Fig. 5B, GFP-Cf9 is a type-1 ($N_{\text{lumen}}-C_{\text{cytosol}}$) chimeric ER membrane protein consisting of the green fluorescent protein linked to the N-terminal *Arabidopsis* chitinase signal peptide and the C-terminal 74 amino acid residues of the tomato *Cladosporium fulvum*-9 (Cf9) disease resistance gene product. This latter region includes a single TMD and a prototypic C-terminal dilysine motif at positions -3 and -4 (underlined, -KKRY-COOH) that has been shown to be essential for

the (steady-state) localization of GFP-Cf9 to the ER [6,32,54]. Fig. 5C shows the results of control experiments in which GFP-Cf9 transiently expressed in onion cells colocalized with co-expressed ss-RFP-HDEL [22], a well-defined ER marker protein consisting of the red fluorescent protein (RFP) fused to an N-terminal signal sequence and the C-terminal -HDEL retrieval signal found in most soluble resident ER proteins. By contrast, replacement of the C-terminal dilysines in GFP-Cf9 with asparagines resulted in this modified GFP-Cf9 (GFP-Cf9ΔN) being mislocalized to the plasma membrane, as evidenced by its colocalization with the co-expressed plasma membrane marker protein RFP-RhoGTPase [7].

Fig. 5C shows also that replacement of the -KKRY motif in GFP-Cf9 with the C-terminal 10 amino acids of *Arabidopsis* GPAT8 resulted in the fusion protein (GFP-Cf9-GPAT8) being localized primarily to the plasma membrane. However, when an additional 16 upstream residues from the GPAT8 protein were included (refer to Fig. 5B), the resulting fusion protein (GFP-Cf9-GPAT8+26) localized entirely to the ER (Fig. 5C). Furthermore, replacement of the dilysine motif at the -1 and -2 positions in the context of this fusion protein (GFP-Cf9-GPAT8+26ΔA) disrupted its ER targeting (Fig. 5C). Taken together, these data indicate that the C-terminal dilysines in GPAT8 are necessary for its ER localization, but, as discussed in more detail below, this sequence motif requires additional upstream residues in order to provide the context for its proper function.

Replacement of the -KKRY motif in GFP-Cf9 with the C-terminal 8 amino acid residues of GPAT9, including the putative pentapeptide ER retrieval motif (-ILARL-) (Fig. 5B), resulted in the fusion protein (GFP-Cf9-GPAT9) being localized entirely to the ER (Fig. 5C). On the other hand, replacement of the pentapeptide motif (-ILARL-) sequence with alanines resulted in the protein (GFP-Cf9-GPAT9ΔA)

being mislocalized to the plasma membrane (Fig. 5C), indicating that the GPAT9 protein relies on this pentapeptide sequence for its steady-state localization in the ER.

Overall, the data presented in Fig. 5 indicate that GPAT8 and GPAT9 possess distinct types of ER retrieval motifs (i.e., dilysine versus hydrophobic pentapeptide motifs). While the functional significance for why these two related proteins possess different ER retrieval signals is not known, similar observations have been reported for other closely related resident ER membrane proteins, e.g., the fatty acid desaturase-2 (FAD2) and FAD3 enzymes also contain distinct ER retrieval motifs at their C-termini [32]. Notably, the presence of different ER retrieval signals in GPAT8 and GPAT9, as well as in FADs, might reflect differences in the interplay between the regulation of their steady-state ER localization and their homo and/or hetero protein–protein interactions, a process that has been described for several other ER membrane proteins that rely on their oligomerization status in order to mediate their localization in plant cells [35].

2.5. Functional divergence of the dilysine ER retrieval motif in GPAT8 proteins

The presence of a divergent dilysine motif at the C terminus of *Arabidopsis* GPAT8 (i.e., –KK–COOH rather than –KKXX–COOH or –KXKXX–COOH) prompted us to investigate whether other members of the GPAT8 protein family also contain a diverged dilysine motif. As shown in Fig. 5A, the majority of GPAT8 proteins do indeed have several lysine residues located within their C-terminal regions, but with the exception of tung (VfGPAT8) and *Physcomitrella patens* (PpGPAT8) proteins (Supplemental Fig. 2), which both end in a prototypic –KKXX–COOH motif, there is no overall conservation in the position of the lysine residues in these sequences. As mentioned above, initial characterizations of the dilysine retrieval motif in mammalian cells revealed that the presence of a lysine residue at the –3 position (e.g., –KKXX or KXKXX) is critical for efficient ER targeting [24,40,53], but the significance of lysine positioning within the dilysine ER retrieval signal in plant cells has not been defined. Consequently, we utilized the apparent divergence of the dilysine residues within the GPAT8 protein family to gain insight to the functionality of this signal in plants.

Towards this end, the GFP-Cf9 reporter protein was employed again to assess whether replacement of the Cf9 C-terminal dilysine motif (–KKRY) with C-terminal sequences from a variety of plant GPAT8 proteins were or were not sufficient in preserving the ER localization of the resulting modified GFP-Cf9 reporter proteins. The results of these experiments are presented in Fig. 6. As expected, the C-terminal sequence from tung GPAT8 including its prototypic dilysine motif (–KKAG–COOH) (Fig. 6A) was sufficient in localizing GFP-Cf9 (GFP-Cf9-VfGPAT8) to the ER, whereas subsequent replacement of the C-terminal lysines with alanines resulted in the modified fusion protein (GFP-Cf9-VfGPAT8ΔA) being mislocalized to the plasma membrane (Fig. 6B). Similarly, the C-terminal sequence from rice GPAT8 (OsGPAT8), despite possessing a diverged dilysine motif (i.e., lysines at the –2 and –4 position, –EKEKN–COOH) (Fig. 6A) was sufficient in localizing GFP-Cf9 (GFP-Cf9-OsGPAT8) to the ER. These latter data, as well as those presented above for the targeting of GFP-Cf9 fused to the *Arabidopsis* GPAT8 C terminus (Fig. 5C), demonstrate that a lysine at the –3 position may not be essential for the dilysine ER retrieval motif to function in plants, although this conclusion needs to be verified by examining the trafficking of other ER membrane proteins possessing dilysine motifs devoid of a lysine at the –3 position.

Fig. 6 shows also that the C-terminal 10 amino acids from potato GPAT8 were not sufficient in sorting GFP-Cf9 to the ER (GFP-Cf9-StGPAT8, Fig. 6A). That is, this fusion protein containing the

diverged dilysine motif (i.e., lysines at the –2 and –3 position) from potato GPAT8 mislocalized to the Golgi, as evidenced by the colocalization of GFP-Cf9-StGPAT8 with the co-expressed Golgi marker protein RFP-Sft11 (Fig. 6B). When an additional eight C-terminal residues upstream of the potato GPAT8 dilysine motif were included, however, the resulting fusion protein (GFP-Cf9-StGPAT8+18) localized entirely to the ER (Fig. 6B), reinforcing the notion that residues upstream of a diverged ER retrieval sequence motif provide the necessary context for its proper functioning. Also notable is that the C-terminal 10 amino acids from pea GPAT8 were sufficient in sorting GFP-Cf9 (GFP-Cf9-PsGPAT8) to the ER (Fig. 6B), suggesting that histidine can replace lysine at the –4 position in the dilysine ER retrieval motif in plants, an observation that is consistent with the functional divergency of the dilysine ER retrieval motif in mammals [21]. Indeed, replacement of the histidine with alanine (GFP-Cf9-PsGPAT8ΔA) (Fig. 6A) abolished ER localization of the reporter protein, and instead, resulted in it being mislocalized to the plasma membrane (Fig. 6B).

Collectively, the results presented in Fig. 6 indicate that the dilysine ER retrieval motif possesses a far greater diversity than that previously proposed for plants [6] and which was based on the original dilysine consensus motif characterized in mammals, i.e., –KXKXX–COOH or –KKXX–COOH [24,40,53]. That is, based on our data, the definition of the plant dilysine ER retrieval motif can be expanded to include additional dilysine combinations at positions –1 and –2, –2 and –3, or –2 and –4, that a lysine at the –4 position within the motif can be replaced by histidine, and that additional residues upstream of the motif are critically important for conveying the proper functional context. Interestingly, results from other recent studies of the dilysine and diarginine ER retrieval motifs in mammals have also led to a growing consensus in the field that these targeting signals are much more diverse than previously believed and need to be redefined, especially in terms of the range of motif variants, their relative position within the protein, and the importance of the subtle differences in the sequence context surrounding the signal with regards to targeting efficiency [17,35,52,61]. Consequently, these ER retrieval motifs appear to be highly complex and the predictive power of previous bioinformatics (computational) searches aimed at identifying candidate ER-resident membrane proteins based on the original consensus motifs for these signals (e.g., the dilysine ER retrieval motif –KKXX–COOH in *Arabidopsis*; [3]) likely needs to be reassessed. For instance, a preliminary survey of the 42 *Arabidopsis* proteins annotated by the Arabidopsis Information Resource and Gene Ontology websites as ‘ER membrane’ revealed that several of these proteins possess C-terminal dilysine combinations that match the expanded definition of the dilysine ER retrieval motif described in this study (Supplemental Table 1).

Our characterization of the divergency of the dilysine ER retrieval motif in plants also permits an analysis of potential ER retrieval signals in other members of the *Arabidopsis* GPAT protein family that were not tested directly in this study. For instance, inspection of the C-termini of *Arabidopsis* GPAT proteins 1–7 (Fig. 1) indicates that GPAT1 lacks any recognizable dilysine motif (or hydrophobic pentapeptide motif), which is consistent with its reported localization in mitochondria [62]. By contrast, the C-termini of GPAT proteins 2–7 all contain several lysine residues, with those in GPAT 2, 3 and 6 being identical to the diverged-type of dilysine motifs described for the GPAT8 proteins from *Arabidopsis* (–KK–COOH), potato (–KKX–COOH) and rice (–KXKX–COOH), respectively (compare C-terminal sequences shown in Figs. 1 and 6A). Whether these dilysine sequences in GPAT 2, 3 and 6 function as *bona fide* ER retrieval signals, however, remains to be experimentally tested and the results of these experiments are significant only if these proteins are demonstrated also to be localized to the ER. Furthermore, although the dilysine

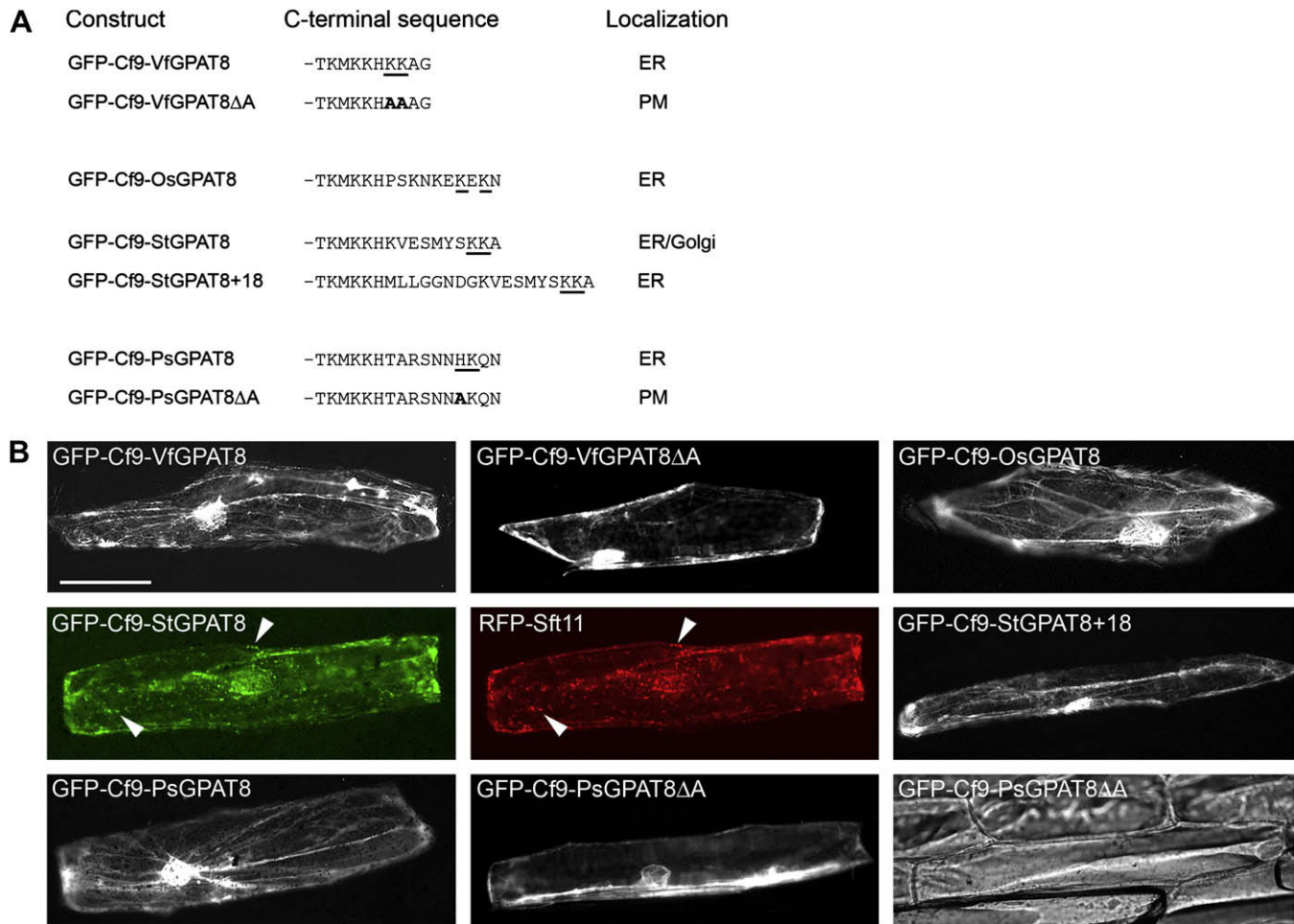


Fig. 6. Mutational analyses of the putative dilysine motifs in various GPAT8 proteins. (A) C-terminal sequences of GFP-Cf9-GPAT8 chimeric proteins and their corresponding intracellular localizations in transformed onion epidermal cells as either ER, ER and Golgi, or plasma membrane (PM). The C-terminal Cf9 sequence was modified by replacing the protein's dilysine motif with various GPAT8 C-terminal sequences, including each protein's putative dilysine ER retrieval motif (underlined). Subsequently mutagenized amino acid residues in these various GFP-Cf9-GPAT8 chimeric proteins are in bold. Tung (Vf), rice (Os), potato (St) and pea (Ps). (B) Onion epidermal peels were transformed transiently with different GFP-Cf9-GPAT8 chimeric proteins as shown in (A) or, for GFP-Cf9-StGPAT8, co-transformed with RFP-Sft11 (consisting of the RFP fused to the N terminus of the *Arabidopsis* Golgi-localized soluble N-ethyl-maleimide sensitive factor attachment protein receptor [SNARE]), serving as a Golgi marker protein [58]. Following bombardment, peels were incubated for ~8 h in the dark and then visualized using either fluorescence or brightfield microscopy. Shown are representative individual onion cells (co-)expressing either GFP-Cf9-VfGPAT8, GFP-Cf9-VfGPAT8ΔA, GFP-Cf9-OsGPAT8, GFP-Cf9-StGPAT8 and RFP-Sft11, GFP-Cf9-StGPAT8+18, GFP-Cf9-PsGPAT8, GFP-Cf9-PsGPAT8ΔA. Shown also is the corresponding brightfield image of the GFP-Cf9-PsGPAT8ΔA-transformed cell. Arrowheads indicate examples of individual Golgi complexes in cells co-transformed with GFP-Cf9-StGPAT8 and RFP-Sft11. Bar = 100 μm.

residues located within the C-termini of *Arabidopsis* GPAT4 (at positions -4 and -6), GPAT5 and GPAT7 (both at positions -11 and -12) (refer to Fig. 1) do not match a prototypic nor a diverged-type dilysine motif, the spectrum of the dilysine motifs will need to be expanded even further if these proteins are indeed shown to be localized in the ER and to utilize their C-terminal dilysine sequences as ER retrieval signals.

3. Conclusions

In this study we characterized the phylogenetic relationships and cellular properties of two members of the *Arabidopsis* GPAT protein family, namely GPAT8, an enzyme involved in cutin biosynthesis [28] and GPAT9, a new putative GPAT which shares homology with a recently identified mammalian GPAT enzyme (GPAT3) that is associated with storage oil formation and, thus, may have a similar role in plants. Protein localization, topology mapping and protein sorting analyses of *Arabidopsis* GPAT8 and GPAT9 demonstrated that these two proteins both localize in the ER and adopt a similar orientation ($N_{\text{cytosol}}-C_{\text{cytosol}}$) in ER membranes, but that they contain

distinct C-terminal ER retrieval signals. Specifically, the GPAT9 protein possesses a hydrophobic pentapeptide ER retrieval motif (-ILARL-) while the GPAT8 protein possesses a divergent dilysine ER retrieval motif (-KK-COOH) that requires additional upstream residues to provide appropriate functional context. These latter data, plus those obtained from functional analyses of other conspicuously divergent dilysine motifs present in GPAT8 proteins from different plant species, led to a considerable expansion of the definition for the consensus dilysine ER retrieval motif in plants.

Overall, the localization of *Arabidopsis* GPAT8 in the ER suggests that at least part of the cutin biosynthetic pathway may take place in this organelle. In a related manner, the localization of *Arabidopsis* GPAT9 in the ER, coupled with the elevated expression pattern observed for this gene during embryogenesis and the sequence homology to mammalian GPAT3, suggests that it might be involved in storage oil formation, although this possibility remains to be tested experimentally. Nonetheless, these studies provide a solid foundation for further exploration of the functional roles of the GPAT gene family in plant glycerolipid metabolism and contribute to our understanding of protein trafficking in plant cells.

4. Materials and methods

4.1. Recombinant DNA procedures and reagents

Standard recombinant DNA procedures were performed as described by Sambrook et al. [47]. Molecular biology reagents were purchased either from New England BioLabs (Beverly, MA), Promega (Madison, WI), Perkin–Elmer (Perkin–Elmer Biosystems, Mississauga, Canada), Stratagene (La Jolla, CA), or Invitrogen (Carlsbad, CA). Oligonucleotides were synthesized by the University of Guelph Laboratory Services (Guelph, Canada) or Invitrogen. DNA was isolated and purified using reagents from Qiagen (Qiagen, Mississauga, Canada) or Promega. All DNA constructs were verified using dye-terminated cycle sequencing performed at the Arizona State University DNA Laboratory (Tempe, Arizona), Mid-South Area Genomics Facility (Jamie Lee Whitten Delta States Research Center, Stoneville, MS) or the University of Guelph Genomics Facility (Guelph, Canada). Mutagenesis was carried out using appropriate complementary forward and reverse mutagenic primers and the QuickChange site-directed mutagenesis kit according to the manufacturer's instructions (Stratagene). A complete list of the sequences of the oligonucleotide primers used in gene identification and plasmid constructions described below is provided in Supplemental Table 2.

4.2. *Arabidopsis* GPAT8 and GPAT9 gene identification and plasmid constructions

Arabidopsis GPAT8 (GenBank accession no. NM_116264) was identified based on BLASTP searches of the deduced *Arabidopsis* proteome using the *Arabidopsis* Information Resource (TAIR) server (<http://www.arabidopsis.org/Blast/index.jsp>) and several of the previously identified *Arabidopsis* GPATs [62] as query sequences. The *Arabidopsis* GPAT8 gene was initially misannotated as two separate genes, At4g00400 and At4g00410. That this region of sequence produced a single mRNA was confirmed by reverse transcriptase (RT)-PCR of total RNA isolated from *Arabidopsis* flowers using GPAT8 gene-specific primers (Supplemental Table 2). The GPAT8 gene has also recently been functionally characterized in *Arabidopsis* and shown to be involved in cutin formation [28]. The entire open reading frame (ORF) of *Arabidopsis* GPAT8 was cloned into the BamHI and Sall sites of pBEVY-L [36] using the “sticky-end” PCR cloning technique [60] and the appropriate primer pairs (Supplemental Table 2), yielding the plasmid pH4 (pBEVY-L/AtGPAT8).

Arabidopsis GPAT9 (GenBank accession no. FJ479752) was identified as a potential GPAT due in part to the presence of an acyltransferase superfamily protein domain (PF01553) as defined by PFAM [15], as well as BLAST analyses with mammalian GPAT3 [9]. The GPAT9 cDNA was cloned by RT-PCR, using gene-specific primers (Supplemental Table 2) for the ORF of the AGI locus At5g60620. The ORF for *Arabidopsis* GPAT9 was then (re)amplified from its original RT-PCR product with gene-specific primers (Supplemental Table 2) which introduced a 5' BamHI site and 3' Sall site. The resulting PCR product was then digested with BamHI and Sall and cloned into the corresponding sites of pBEVY-L, yielding the plasmid pH22 (pBEVY-L/AtGPAT9).

Plant expression plasmids containing N- or C-terminal myc-epitope-tagged versions of *Arabidopsis* GPAT8 and GPAT9 were constructed in the following manner. First, the *Arabidopsis* GPAT8 and GPAT9 ORFs were amplified from pH4 and pH22 (see above), respectively, using the PCR along with appropriate forward and reverse primers that introduced XbaI and NheI sites immediately 5' and 3' of their start and stop codons, respectively. Next, PCR products were gel-purified and subcloned into XbaI–NheI-digested

pRTL2/myc-MCS, yielding pRTL2/myc-GPAT8 and pRTL2/myc-GPAT9. pRTL2/myc-MCS [54] is a modified version of the plant expression vector pRTL2ΔN/S [26] containing the 35S cauliflower mosaic virus promoter and sequences encoding an initiation methionine, glycine linkers and the myc-epitope tag (underlined, MGEQKLISEEDLG–; [16]). To construct pRTL2/GPAT8-myc and pRTL2/GPAT9-myc, the GPAT8 and GPAT9 ORFs were amplified using PCR and pH4 and pH22, respectively, as template DNA. Forward and reverse primers used in these PCRs introduced an in-frame XbaI site 5' of the GPAT8 or GPAT9 start codon and an NcoI site immediately 5' of each stop codon. The resulting PCR products were digested with XbaI and NcoI and ligated into XbaI–NcoI-digested pRTL2/X-myc, a modified version of pRTL2ΔN/S with sequences encoding XbaI, NheI and NcoI sites followed by a myc-epitope tag and stop codon [54].

The construction of pRTL2/GFP-Cf9 and pRTL2/GFP-Cf9ΔN has been described previously [32]. All plasmids coding for GFP-Cf9 mutants with altered amino acid residues at the C terminus of Cf9 (Figs. 5 and 6) were constructed using site-directed PCR mutagenesis with pRTL2/GFP-Cf9 as template DNA and the appropriate complementary forward and reverse mutagenic primers (see Supplemental Table 2). Details on the construction of pRTL2/RFP-HDEL (encoding RFP fused to the N-terminal *Arabidopsis* chitinase signal sequence and C-terminal –HDEL ER retrieval signal), pRTL2/RFP-Rac3 (encoding RFP fused to the *Arabidopsis* RhoGTPase Rac3), and pRTL2/Sft11 (encoding RFP fused to the N terminus of the *Arabidopsis* SNARE Sft11 and previously referred to as pRTL2/BS14a) have been described previously [54].

4.3. Bioinformatics analysis

All known or predicted GPAT sequences described in this study were compared using WWW-based BLAST algorithm programs [1]. Phylogenetic comparisons were carried out by generation of multiple sequence alignments using the CLUSTALX program (version 1.8) (www.clustal.org) and its default settings. Dendrograms were created from the alignments using the neighbor joining method [46] in the TreeView program [42]. Predicted transmembrane domains (TMDs) in GPAT proteins were identified using the TMHMM Server (version 2.0) (<http://www.cbs.dtu.dk/services/TMHMM>) and visual inspection.

Publicly available *Arabidopsis* microarray expression datasets were explored for the *Arabidopsis* GPAT genes using the tools available through the BioArray Resource (BAR) Expression Profiler (http://bar.utoronto.ca/affydb/cgi-bin/affy_db_exprss_browser_in.cgi) [57]. Output from the extended tissue series dataset was formatted into a heat map using the DataMetaFormatter tool as hosted at the BAR website (http://bar.utoronto.ca/ntools/cgi-bin/ntools_treeview_word.cgi). Expression patterns in different tissues were expressed as averages of replicate log-transformed values normalized to the averages of the appropriate controls.

All other sequences included are predicted proteins found by TBLASTN analyses using the TIGR (The Institute for Genomic Research) Plant Transcript Assemblies BLAST server (http://blast.jcvi.org/euk-blast/plantta_blast.cgi) representing GPAT8 and GPAT9 sequences from *Populus trichocarpa* (PtGPAT8, transcript assembly TA18743_3694), potato (*Solanum tuberosum*, StGPAT8, TA27769_4113; StGPAT9, TA28820_4113), *Aquilegia shockleyi* (AsGPAT8, TA9909_338618), *Gossypium raimondii* (GrGPAT8, TA10351_29730; GrGPAT9, TA13765_29730), corn (*Zea mays*, ZmGPAT8, TA173221_4577; ZmGPAT9 TA160402_4577), rice (*Oryza sativa*, OsGPAT8, TA44887_4530; OsGPAT9, TA44369_4530), castor bean (*Ricinus communis*, GenBank accession no. EU391594), *P. patens* (PpGPAT8, predicted protein EDQ81824, [45]), *Vitis vinifera* (VvGPAT8, TA36577_29760; VvGPAT9, TA36407_29760), pea (*Pisum sativum*,

PsGPAT8, TA7916_3352; PsGPAT9, TC60295), barley (*Hordeum vulgare*, HvGPAT9, TA35530_4513), wheat (*Triticum aestivum*, TaGPAT9, TA73724_4565), tomato (*Lycopersicon esculentum*, LeGPAT9, TC187111 and TC176075), lettuce (*Lactuca sativa*, LsGPAT9, TA2637_4236), sunflower (*Helianthus annuus*, HaGPAT9, TA14377_4232), *Helianthus exilis* (HeGPAT9, TA1057_400408), tung (*V. fordii*, VfGPAT8, GenBank accession no. FJ479753; VfGPAT9, GenBank accession no. FJ479751) and *Brassica oleracea* (BoGPAT9, TA8243_3712).

4.4. Transient transformation of tobacco suspension cells and onion epidermal cells, and fluorescence microscopy

Tobacco (*N. tabacum* cv Bright Yellow-2 [BY-2]) suspension-cultured cells were maintained and prepared for biolistic bombardment as described previously [4]. Briefly, transient transformations were performed using 5 µg of plasmid DNA (or 2.5 µg of each plasmid for co-transformations) with a biolistic particle delivery system-1000/HE (Bio-Rad Laboratories, Mississauga, Canada). Bombarded cells were incubated for ~4 h to allow for expression and sorting of the introduced gene product(s), then fixed in formaldehyde, and incubated with 0.01% (w/v) pectolyase Y-23 (Kyowa Chemical Products, Osaka, Japan). Thereafter, cells were (differentially) permeabilized with either 0.3% (v/v) triton X-100 or 25 µg ml⁻¹ digitonin (Sigma–Aldrich Ltd.) [26]. Cells were evaluated after ~4 h to ensure that any potential negative effects due to (membrane) protein over-expression were diminished.

Primary and secondary antibody sources were as follows: mouse anti-myc antibodies in hybridoma medium (clone 9E10; Princeton University, Monoclonal Antibody Facility, Princeton, NJ); rabbit anti-E1β [29] (kindly provided by Jan Miernyk); rabbit anti-calreticulin (kindly provided by Sean Coughlan); mouse anti-α-tubulin (Sigma–Aldrich Ltd.); goat anti-mouse Alexa Fluor 488 IgGs (Cedar Lane Laboratories, Ontario, Canada); goat anti-rabbit rhodamine red-X IgGs (Jackson ImmunoResearch Laboratories, West Grove, PA). ConA conjugated to Alexa 594 (Molecular probes, Eugene, OR) was added to BY-2 cells at a final concentration of 5 µg ml⁻¹ during the final 20 min of incubation with secondary antibodies.

Transient transformation of onion epidermal cells was carried out as described by McCartney et al. [32]. Onions were purchased at a local greengrocer (Guelph, Canada) and bombardments were performed with 10 µg of plasmid DNA or 5 µg of each plasmid for co-transformations. Approximately 8 h after bombardment, peels were mounted onto glass slides without a cover slip and GFP and RFP signals were analyzed via fluorescence microscopy.

Microscopic (fluorescence, brightfield and differential interference contrast [DIC]) images of BY-2 and onion cells were acquired using a Zeiss Axioskop 2 MOT epifluorescence microscope (Carl Zeiss, Toronto, Canada) with a Zeiss 63× Plan Apochromat oil-immersion objective lens. Image captures were performed using a Retiga 1300 charge-coupled device camera (Qimaging, Burnaby, Canada) and OpenLab 5.0 (Improvision Inc., Lexington, MA, USA). All images of cells shown were deconvolved and adjusted for brightness and contrast using Northern Eclipse 5.0 software (Empix Imaging, Mississauga, Canada) and are representative of >50 independent (transient) transformations from at least two independent transformation experiments. Figure compositions were generated using Adobe Photoshop CS (Adobe Systems, San Jose, CA).

Acknowledgements

This work was supported by the United States Department of Agriculture, Current Research Information System (CRIS) project numbers 5347-21410-005-00D and 5347-21000-009-00D to JMD,

CRIS project no. 6435-41000-087-00D to JMS, and a grant from the Natural Sciences and Engineering Research Council (NSERC) (grant no. 217291) to RTM. Financial support for SKG was provided by funds from the Ontario Research and Development Challenge Fund (Ontario Center for Agriculture Genomics) (grant no. 046061) to SJR. We gratefully thank Dr. Daphne Goring (University of Toronto) for assistance with the electronic expression profiling of the GPAT family and Dr. Daiyuan Zhang (United States Department of Agriculture) for her comments during the writing of the manuscript.

Appendix. Supplementary data

Supplementary data associated with this article can be found, in the online version, at doi:10.1016/j.plaphy.2009.05.008.

References

- [1] S.F. Altschul, T.L. Madden, A.A. Schaffer, J. Zhang, Z. Zhang, W. Miller, D.J. Lipman, Gapped BLAST and PSI-BLAST: a new generation of protein database search programs, *Nucleic Acids Res.* 25 (1997) 3389–3402.
- [2] K. Athenstaedt, S. Weys, F. Paltauf, G. Daum, Redundant systems of phosphatidic acid biosynthesis via acylation of glycerol-3-phosphate or dihydroxyacetone phosphate in the yeast *Saccharomyces cerevisiae*, *J. Bacteriol.* 181 (1999) 1458–1463.
- [3] R.S. Austin, N.J. Provart, S.R. Cutler, C-terminal motif prediction in eukaryotic proteomes using comparative genomics and statistical over-representation across protein families, *BMC Genomics* 8 (2007) 191.
- [4] A. Banjoko, R.N. Trelease, Development and application of an in vivo plant peroxisome import system, *Plant Physiol.* 107 (1995) 1201–1208.
- [5] F. Beisson, Y. Li, G. Bonaventure, M. Pollard, J.B. Ohlrogge, The acyltransferase GPAT5 is required for the synthesis of suberin in seed coat and root of *Arabidopsis*, *Plant Cell* 19 (2007) 351–368.
- [6] M. Benghezal, G.O. Wasteneys, D.A. Jones, The C-terminal dilysine motif confers endoplasmic reticulum localization to type I membrane proteins in plants, *Plant Cell* 12 (2000) 1179–1201.
- [7] F. Bischoff, L. Vahlkamp, A. Molendijk, K. Palme, Localization of AtROP4 and AtROP6 and interaction with the guanine nucleotide dissociation inhibitor AtRhoGDI1 from *Arabidopsis*, *Plant Mol. Biol.* 42 (2000) 515–530.
- [8] F. Brandizzi, S. Irons, A. Kearns, C. Hawes, BY-2 cells: culture and transformation for live-cell imaging, *Curr. Protoc. Cell Biol.* (2003) (Chapter 1), Unit 1.7.
- [9] J. Cao, J.-L. Li, D. Li, J.F. Tobin, R.E. Gimeno, Molecular identification of microsomal acyl-CoA:glycerol-3-phosphate acyltransferase, a key enzyme in *de novo* triacylglycerol synthesis, *Proc. Natl. Acad. Sci. U.S.A.* 103 (2006) 19695–19700.
- [10] F.S. Cordes, J.N. Bright, M.S.P. Sansom, Proline-induced distortions of transmembrane helices, *J. Mol. Biol.* 323 (2002) 951–960.
- [11] P. Cosson, Y. Lefkir, C. Démollière, F. Letourneur, New COP1-binding motifs involved in ER retrieval, *EMBO J.* 17 (1998) 6863–6870.
- [12] P. Dörmann, C. Benning, Galactolipids rule in seed plants, *Trends Plant Sci.* 7 (2002) 112–118.
- [13] J.M. Dyer, D.C. Chapital, J.C. Kuan, R.T. Mullen, C. Turner, T.A. McKeon, A.B. Pepperman, Molecular analysis of a bifunctional fatty acid conjugase/desaturase from tung. Implications for the evolution of plant fatty acid diversity, *Plant Physiol.* 130 (2002) 2027–2038.
- [14] J.M. Dyer, R.T. Mullen, Immunocytological localization of two plant fatty acid desaturases in the endoplasmic reticulum, *FEBS Lett.* 494 (2001) 44–47.
- [15] R.D. Finn, J. Tate, J. Mistry, P.C. Coggill, S.J. Sammut, H.R. Hotz, G. Ceric, K. Forslund, S.R. Eddy, E.L. Sonnhammer, A. Bateman, The Pfam protein families database, *Nucleic Acids Res.* 36 (2008) D281–D288.
- [16] C.E. Fritze, T.R. Anderson, Epitope tagging: general method for tracking recombinant proteins, *Methods Enzymol.* 327 (2000) 3–16.
- [17] M. Gassmann, C. Haller, Y. Stoll, S.A. Aziz, B. Biermann, J. Mosbacher, K. Kaupmann, B. Bettler, The RXR-type endoplasmic reticulum-retention/retrieval signal of GABAB1 requires distant spacing from the membrane to function, *Mol. Pharmacol.* 68 (2005) 137–144.
- [18] R.E. Gimeno, J. Cao, Mammalian glycerol-3-phosphate acyltransferases: new genes for an old activity, *J. Lipid Res.* 49 (2008) 2079–2088.
- [19] V. Gomord, E. Wee, L. Faye, Protein retention and localization in the endoplasmic reticulum and the Golgi apparatus, *Biochimie* 81 (1999) 607–618.
- [20] M.R. Gonzalez-Baro, D.A. Granger, R.A. Coleman, Mitochondrial glycerol phosphate acyltransferase contains two transmembrane domains with the active site in the N-terminal domain facing the cytosol, *J. Biol. Chem.* 276 (2001) 43182–43188.
- [21] B. Hardt, E. Bause, Lysine can be replaced by histidine but not by arginine as the ER retrieval motif for type I membrane proteins, *Biochem. Biophys. Res. Commun.* 291 (2002) 751–757.
- [22] J. Haseloff, K.R. Siemering, D.C. Prasher, S. Hodge, Removal of a cryptic intron and subcellular localization of green fluorescent protein are required to mark transgenic *Arabidopsis* plants brightly, *Proc. Natl. Acad. Sci. U.S.A.* 94 (1997) 2122–2127.

- [23] Y.T. Hwang, S.M. Pelitire, M.P. Henderson, D.W. Andrews, J.M. Dyer, R.T. Mullen, Novel targeting signals mediate the sorting of different isoforms of the tail-anchored membrane protein cytochrome *b*₅ to either endoplasmic reticulum or mitochondria, *Plant Cell* 16 (2004) 3002–3019.
- [24] M.R. Jackson, T. Nilsson, P.A. Peterson, Identification of a consensus motif for retention of transmembrane proteins in the endoplasmic reticulum, *EMBO J.* 9 (1990) 3153–3162.
- [25] M.C. Lee, E.A. Miller, J. Goldberg, L. Orci, R. Schekman, Bi-directional protein transport between the ER and Golgi, *Annu. Rev. Cell Dev. Biol.* 20 (2004) 87–123.
- [26] M.S. Lee, R.T. Mullen, R.N. Trelease, Oilseed isocitrate lyases lacking their essential type-1 peroxisomal targeting signal are piggybacked to glyoxysomes, *Plant Cell* 9 (1997) 185–197.
- [27] T.M. Lewin, P. Wang, R.A. Coleman, Analysis of amino acid motifs diagnostic for the *sn*-glycerol-3-phosphate acyltransferase reaction, *Biochemistry* 38 (1999) 5764–5771.
- [28] Y. Li, F. Beisson, A.J.K. Koo, I. Molina, M. Pollard, J. Ohlrogge, Identification of acyltransferases required for cutin biosynthesis and production of cutin with suberin-like monomers, *Proc. Natl. Acad. Sci. U.S.A.* 104 (2007) 18339–18344.
- [29] M.H. Luethy, J.A. Miernyk, D.D. Randall, The mitochondrial pyruvate dehydrogenase complex: nucleotide and deduced amino-acid sequences of a cDNA encoding the *Arabidopsis thaliana* E1 alpha-subunit, *Gene* 164 (1995) 251–254.
- [30] A. Mallabiabarrena, M. Fresno, B. Alarcón, An endoplasmic reticulum retention signal in the CD3 epsilon chain of the T-cell receptor, *Nature* 357 (1992) 593–596.
- [31] A. Mallabiabarrena, M.A. Jiménez, M. Rico, B. Alarcón, A tyrosine-containing motif mediates ER retention of CD3-epsilon and adopts α helix-turn structure, *EMBO J.* 14 (1995) 2257–2268.
- [32] A.W. McCartney, J.M. Dyer, P.K. Dhanoa, P.K. Kim, D.W. Andrews, J.A. McNew, R.T. Mullen, Membrane-bound fatty acid desaturases are inserted co-translationally into the ER and contain different ER retrieval motifs at their carboxy termini, *Plant J.* 37 (2004) 156–173.
- [33] H.T. McMahon, I.G. Mills, COP and clathrin-coated vesicle budding: different pathways, common approaches, *Curr. Opin. Cell Biol.* 16 (2004) 379–391.
- [34] Y.S. Miao, L. Jiang, Transient expression of fluorescent fusion proteins in protoplasts of suspension cultured cells, *Nat. Protoc.* 2 (2007) 2348–2353.
- [35] K. Michelsen, H. Yuan, B. Schwappach, Hide and run. Arginine-based endoplasmic-reticulum-sorting motifs in the assembly of heteromultimeric membrane proteins, *EMBO Rep.* 6 (2005) 717–722.
- [36] C.A. Miller 3rd, M.A. Martinat, L.E. Hyman, Assessment of aryl hydrocarbon receptor complex interactions using pBEVY plasmids: expression vectors with bi-directional promoters for use in *Saccharomyces cerevisiae*, *Nucleic Acids Res.* 26 (1998) 3577–3583.
- [37] R.T. Mullen, C.S. Lisenbee, C.R. Flynn, R.N. Trelease, Stable and transient expression of chimeric peroxisomal membrane proteins induces an independent “zippering” of peroxisomes and an endoplasmic reticulum subdomain, *Planta* 213 (2001) 849–863.
- [38] N. Murata, Y. Tasaka, Glycerol-3-phosphate acyltransferase in plants, *Biochim. Biophys. Acta* 1348 (1997) 10–16.
- [39] T. Nagata, Y. Nemoto, S. Hasezawa, Tobacco BY-2 cell line as the “Hela” cell in the cell biology of higher plants, *Int. Rev. Cytol.* 132 (1992) 1–30.
- [40] T. Nilsson, M. Jackson, P.A. Peterson, Short cytoplasmic sequences serve as retention signals for transmembrane proteins in the endoplasmic reticulum, *Cell* 58 (1989) 707–718.
- [41] J. Ohlrogge, J. Browse, Lipid biosynthesis, *Plant Cell* 7 (1995) 957–970.
- [42] R.D. Page, TreeView: an application to display phylogenetic trees on personal computers, *Comput. Appl. Biosci.* 12 (1996) 357–358.
- [43] H. Pelham, Getting stuck in the Golgi, *Traffic* 1 (2000) 191–192.
- [44] M. Pellon-Maison, R.A. Coleman, M.R. Gonzalez-Bar, The C-terminal region of mitochondrial glycerol-3-phosphate acyltransferase-1 interacts with the active site region and is required for activity, *Arch. Biochem. Biophys.* 450 (2006) 157–166.
- [45] S.A. Rensing, D. Lang, A.D. Zimmer, A. Terry, A. Salamov, H. Shapiro, T. Nishiyama, P.F. Perroud, E.A. Lindquist, Y. Kamisugi, T. Tanahashi, K. Sakakibara, T. Fujita, K. Oishi, T. Shin-I, Y. Kuroki, A. Toyoda, Y. Suzuki, S. Hashimoto, K. Yamaguchi, S. Sugano, Y. Kohara, A. Fujiyama, A. Anterola, S. Aoki, N. Ashton, W.B. Barbazuk, E. Barker, J.L. Bennetzen, R. Blankenship, S.H. Cho, S.K. Dutcher, M. Estelle, J.A. Fawcett, H. Gundlach, K. Hanada, A. Heyl, K.A. Hicks, J. Hughes, M. Lohr, K. Mayer, A. Melkozernov, T. Murata, D.R. Nelson, B. Pils, M. Prigge, B. Reiss, T. Renner, S. Rombauts, P.J. Rushton, A. Sanderfoot, G. Schween, S.H. Shiu, K. Stueber, F.L. Theodoulou, H. Tu, Y. Van de Peer, P.J. Verrier, E. Waters, A. Wood, L. Yang, D. Cove, The *Physcomitrella* genome reveals evolutionary insights into the conquest of land by plants, *Science* 319 (2007) 64–69.
- [46] N. Scitou, M. Nei, The neighbor-joining method: a new method for reconstructing phylogenetic trees, *Mol. Biol. Evol.* 4 (1987) 406–425.
- [47] J. Sambrook, E.F. Fritsch, T. Maniatis, *Molecular Cloning: a Laboratory Manual*, second ed. Cold Spring Harbor Laboratory Press, Cold Spring Harbor, NY, 1989.
- [48] M. Schmid, T.S. Davison, S.R. Henz, U.J. Pape, M. Demar, M. Vingron, B. Schölkopf, D. Weigel, J. Lohmann, A gene expression map of *Arabidopsis* development, *Nat. Genet.* 37 (2005) 501–506.
- [49] T.U. Schwartz, Origins and evolution of cotranslational transport to the ER, *Adv. Exp. Med. Biol.* 607 (2007) 52–60.
- [50] N. Scitou, S. Wyatt, P.-L. Tsou, D. Robertson, N. Strömberg Allen, Model system for plant cell biology: GFP imaging in living onion epidermal cells, *Biotechniques* 26 (1999) 1125–1132.
- [51] S.O. Shan, P. Walter, Co-translational protein targeting by the signal recognition particle, *FEBS Lett.* 579 (2005) 921–926.
- [52] S. Shikano, M. Li, Membrane receptor trafficking: evidence of proximal and distal zones conferred by two independent endoplasmic reticulum localization signals, *Proc. Natl. Acad. Sci. U.S.A.* 100 (2003) 5783–5788.
- [53] J. Shin, R.L. Dunbrack Jr., S. Lee, J.L. Strominger, Signals for retention of transmembrane proteins in the endoplasmic reticulum studied with CD4 truncation mutants, *Proc. Natl. Acad. Sci. U.S.A.* 88 (1991) 1918–1922.
- [54] J.M. Shockey, S.K. Gidda, D.C. Chapital, J.C. Kuan, J.M. Bland, S.J. Rothstein, R.T. Mullen, J.M. Dyer, Tung tree DGAT1 and DGAT2 have nonredundant functions in triacylglycerol biosynthesis and are localized to different subdomains of the endoplasmic reticulum, *Plant Cell* 18 (2006) 2294–2313.
- [55] A.M. Tartakoff, P. Vassalli, Lectin-binding sites as markers of Golgi sub-compartments: proximal-to-distal maturation of oligosaccharides, *J. Cell Biol.* 97 (1983) 1243–1248.
- [56] R.D. Teasdale, M.R. Jackson, Signal-mediated sorting of membrane proteins between the endoplasmic reticulum and the Golgi apparatus, *Annu. Rev. Cell Dev. Biol.* 12 (1996) 27–54.
- [57] K. Toufighi, S.M. Brady, R. Austin, E. Ly, N.J. Provart, The Botany Array Resource: e-Northern, expression angling, and promoter analyses, *Plant J.* 43 (2005) 153–163.
- [58] T. Uemura, T. Ueda, R.L. Ohniwa, A. Nakano, K. Takeyasu, M.H. Sato, Systematic analysis of SNARE molecules in *Arabidopsis*: dissection of the post-Golgi network in plant cells, *Cell Struct. Funct.* 29 (2004) 49–65.
- [59] W.O. Wilkison, R.M. Bell, *sn*-Glycerol-3-phosphate acyltransferase from *Escherichia coli*, *Biochim. Biophys. Acta* 1348 (1997) 3–9.
- [60] G. Zeng, Sticky-end PCR: new method for subcloning, *Biotechniques* 25 (1998) 206–208.
- [61] N. Zerangue, M.J. Malan, S.R. Fried, P.F. Dazin, Y.N. Jan, L.Y. Jan, B. Schwappach, Analysis of endoplasmic reticulum trafficking signals by combinatorial screening in mammalian cells, *Proc. Natl. Acad. Sci. U.S.A.* 98 (2001) 2431–2436.
- [62] Z. Zheng, Q. Xia, M. Daux, W. Shen, G. Selvaraj, J. Zou, *Arabidopsis* AtGPAT1, a member of the membrane-bound glycerol-3-phosphate acyltransferase gene family, is essential to tapetum differentiation and male fertility, *Plant Cell* 15 (2003) 1872–1887.
- [63] Z. Zheng, J. Zou, The initial step of the glycerolipid pathway. Identification of glycerol-3-phosphate/dihydroxyacetone phosphate dual substrate acyltransferases in *Saccharomyces cerevisiae*, *J. Biol. Chem.* 276 (2001) 41710–41716.